IEEE Access
Multidisciplinary ⋮ Rapid Review ⋮ Open Access Journal

Received March 2, 2021, accepted April 8, 2021, date of publication April 12, 2021, date of current version April 20, 2021.

Digital Object Identifier 10.1109/ACCESS.2021.3072550

Optimal Operation Strategy of Virtual Power Plant Considering Real-Time Dispatch Uncertainty of Distributed Energy Resource Aggregation

JINHO LEE AND DONGJUN WON

Department of Electrical and Computer Engineering, Inha University, Incheon 22212, South Korea

Corresponding author: Dongjun Won (djwon@inha.ac.kr)

This work was supported in part by the Korea Institute of Energy Technology Evaluation and Planning (KETEP) and the Ministry of Trade, Industry & Energy (MOTIE) of the Republic of Korea (No. 20194310100030), and in part by the Energy Cloud Research and Development Program through the National Research Foundation of Korea (NRF) funded by the Ministry of Science and ICT under Grant 2019M3F2A1073.

ABSTRACT Virtual power plant (VPP) technologies continue to develop to embrace various types of distributed energy resources (DERs) that have inherent real-time uncertainty. To prevent side effects on the power system owing to the uncertainty, the VPP should manage its internal resources' uncertainty as a whole. This paper proposes an optimal operation strategy for a VPP participating in day-ahead and real-time energy market so that a distributed energy resource aggregation (DERA) can cope with real-time fluctuation due to uncertainties while achieving its maximum profit. The proposed approach has bidding models of the DERAs including microgrid, electric vehicle aggregation, and demand response aggregation, as well as the VPP. The VPP determines internal prices applied to the DERA by evaluating its real-time responses to the day-ahead schedule and updating proposed pricing function parameters, and the DERA adjusts its energy reserves. By repeating this coordination process, the VPP can establish an optimal operation strategy to manage real-time uncertainty on the DERA's own. The effectiveness of the proposed strategy is verified by identifying a capability of the DERA to cope with real-time fluctuation through scenario-based simulations. The result shows that the VPP can reduce 1.6% of cost while the internal price applied to the DERA is close to the maximum.

INDEX TERMS Virtual power plant, distributed energy resource aggregation, electricity market, uncertainty, real-time dispatch.

NOMENCLATURE

A. SET AND INDICES

c	*VPP participant classification code (PV, ESS, EVA, DRA, MG)*
i	*number index of participants*
N	*total number of participants*
T	*total scheduling time*
Δt	*scheduling time interval*
k	*index of k-th day*
$\widehat{PV}$	*set of PVs participating in VPP*
$\widehat{ESS}$	*set of ESSs participating in VPP*
$\widehat{EVA}$	*set of EVAs participating in VPP*
$\widehat{DRA}$	*set of DRAs participating in VPP*
$\widehat{MG}$	*set of MGs participating in VPP*

B. PARAMETERS

$\pi^s_{DA}(t)/\pi^s_{RT}(t)$	*Energy selling price in day-ahead market (DAM)/ real-time market (RTM) at time t*
$\pi^b_{DA}(t)/\pi^b_{RT}(t)$	*Energy purchasing price in DAM/RTM*
$P^c_{DAbid,i}(t)$ / $P^c_{RTbid,i}(t)$	*Energy bid of i-th participant c in DAM/RTM at time* $t(\forall c \in \widehat{PV})$
$P^c_{DAload,i}(t)/P^c_{RTload,i}(t)$	*Forecasted load of i-th participant c in DAM/RTM at time t*

The associate editor coordinating the review of this manuscript and approving it for publication was Jiayong Li.

$P^{c}_{DAsche,i}(t)$ / $P^{c}_{RTsche,i}(t)$ — *Schedule reference of i-th participant c in DAM/RTM at time t*

η^{c}_{i} — *ESS charging and discharging efficiency of i-th participant c*

Cap^{c}_{i} — *ESS battery capacity of i-th participant c*

$SOC^{c,ini}_{i}$ / $SOC^{c,end}_{i}$ — *ESS initial/final state of charge (SOC) of i-th participant c*

$SOC^{c,lb}_{i}$ / $SOC^{c,ub}_{i}$ — *ESS SOC lower/upper bound of i-th participant c*

$P^{VPP,b,max}_{DAbid}(t)$ / $P^{VPP,b,max}_{RTbid}(t)$ — *Upper bound of purchasing bid of VPP in DAM/RTM at time t*

$P^{VPP,s,max}_{DAbid}(t)$ / $P^{VPP,s,max}_{RTbid}(t)$ — *Upper bound of selling bid of VPP in DAM/RTM at time t*

$P^{c,min}_{DAbid,i}(t)$/ $P^{c,min}_{RTbid,i}(t)$ — *Lower bound of bid of i-th participants c in DAM/RTM at time t*

$P^{c,max}_{DAbid,i}(t)$/ $P^{c,max}_{RTbid,i}(t)$ — *Upper bound of bid of i-th participant c in DAM/RTM at time t*

$P^{c,ch,max}_{DAbid,i}(t)$ / $P^{c,dch,max}_{DAbid,i}(t)$ — *Upper bound of battery charging and discharging of i-th participants c in DAM at time t*$(\forall c \in \widehat{ESS})$

$P^{c,ch,max}_{RTbid,i}(t)$ / $P^{c,dch,max}_{RTbid,i}(t)$ — *Upper bound of battery charging and discharging of i-th participants c in RTM at time t*$(\forall c \in \widehat{ESS})$

$C^{c}_{i}(t)$ — *Pricing function of i-th participant c at time t*

$\gamma^{c}_{i}(t)$ — *Error rate between DAM bid and RTM response of i-th participant c at time t*

$\pi^{s}_{wh}(t)/\pi^{s}_{re}(t)$ — *Selling price in wholesale/retail market at time t*

$\pi^{b}_{wh}(t)/\pi^{b}_{re}(t)$ — *Purchasing price in wholesale/retail market at time t*

$P^{c}_{RT,i}(t)$ — *Real-time power of i-th participant c*

E_{MG} — *Sum of DAM MG reserve in real-time environment (for 24 h per 5 min)*

C. VARIABLES

$P^{VPP,s}_{DAbid}(t)$/ $P^{VPP,s}_{RTbid}(t)$ — *Selling bid of VPP in DAM/RTM at time t*

$P^{VPP,b}_{DAbid}(t)$/ $P^{VPP,b}_{RTbid}(t)$ — *Purchasing bid of VPP in DAM/RTM at time t*

$P^{c}_{DAbid,i}(t)$ / $P^{c}_{RTbid,i}(t)$ — *Energy bid of i-th participant c in DAM/RTM at time t* $(\forall c \in \widehat{ESS}, \widehat{EVA}, \widehat{DRA}, \widehat{MG})$

$P^{c,ch}_{DAbid,i}(t)$/ $P^{c,dch}_{DAbid,i}(t)$ — *Charge/discharge energy of i-th participants c in DAM at time t* $(\forall c \in \widehat{ESS})$

$\mu^{c,ch}_{DA,i}(t)$/ $\mu^{c,dch}_{DA,i}(t)$ — *Binary variable of battery charging / discharging in DAM at time t* $(\forall c \in \widehat{ESS})$

$P^{c,ch}_{RTbid,i}(t)$/ $P^{c,dch}_{RTbid,i}(t)$ — *Charge/discharge energy of i-th participants c in RTM at time t* $(\forall c \in \widehat{ESS})$

$\mu^{c,ch}_{RT,i}(t)/\mu^{c,dch}_{RT,i}(t)$ — *Binary variable of battery charging / discharging in RTM at time t* $(\forall c \in \widehat{ESS})$

$SOC^{c}_{i}(t)$ — *ESS SOC of i-th participant c at time t*

$\mu^{b}_{DA}(t)$ / $\mu^{b}_{RT}(t)$ — *Binary variable of purchase in DAM/RTM at time t*

$\mu^{s}_{DA}(t)/\mu^{s}_{RT}(t)$ — *Binary variable of sales in DAM/RTM at time t*

I. INTRODUCTION

Renewable energy sources are consistently deployed in the power generation sector to reduce greenhouse gas emissions, which is the main cause of climate change. As of 2018, modern renewable energy accounts for 11 % of the world's final energy consumption and continues to increase [1]. In Korea, the government aims to expand the portion of renewable energy from 7 % of the total power generation to 20 % by 2030 under the 3020 renewable energy policy. Most of the renewable energy corresponding to this goal is solar and wind power. Solar and wind energy account for 57 % and 28 % of the capacity goals, respectively [2]. However, uncertainties inherent in distributed energy sources (DERs) such as solar and wind power can adversely affect power supply plans from an energy perspective and worsen the power quality from a power perspective. To address these problems, a virtual power plant (VPP) is being developed [3]. VPP aims to contribute to the supply and demand balance at the transmission system level through direct participation in the power market [4], [5].

Resources in the VPP consist of power generating units, power utilization units, power storage units, and microgrids (MGs), as shown in Fig. 1 [6]. According to [7], the aggregation of DERs such as energy storage, distributed generation, demand response, energy efficiency, and electric vehicles connected to the distribution network are allowed

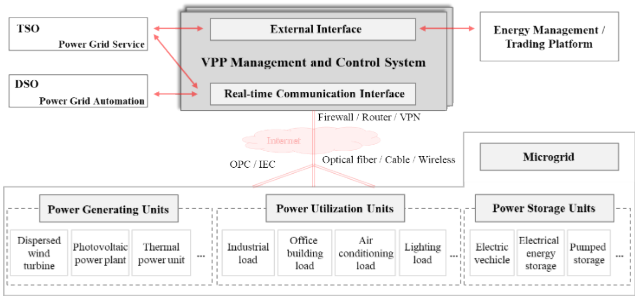

FIGURE 1. VPP system composition diagram.

to participate in the power market. For a VPP with inherent uncertainties to obtain maximum profits in the power market, a bid scheduling when considering the uncertainties and their countermeasures, as well as a strategy to minimize purchase or sales in a real-time market (RTM), is required [8] because the purchase price in RTM is generally higher than that in the day-ahead market (DAM) and the sales price is cheaper than in DAM [9].

Optimal operation strategies of VPP participating in power markets considering uncertainties have been studied in many literatures [8]. However, they have rarely addressed aggregation resources participating in the VPP, and penalties for each resource with regard to not properly responding day-ahead schedule in real-time environment. In [10], a problem for minimizing cost of MGs integrated with renewable energy resources have been solved using binary particle swarm optimization. In [11], a joint day-ahead and real-time market for VPP with DR model has been constructed using a two-level robust optimization model to minimize penalty in real-time market considering an uncertainty margin. Authors in [12] have presented a hybrid optimization model including grid search algorithm and a proprietary derivative-free algorithm for DGs, ESSs, and MGs in VPP. A DAM bidding strategy for a VPP as a price maker to minimize RTM penalty has been studied through uncertain resources modeling using interval interpretation [13]. A strategy for a VPP to purchase DR services to reduce penalty cost has been presented in [14]. The problem is formulated as multistage stochastic optimization model, which is a time order.

A study using fuzzy optimization techniques considering the uncertainty of renewable energy can be found in [15]. The VPP trades energy and DR internally with consumers in its territory based on demand curtailment requests. Authors of [16] proposed a self-scheduling strategy using a multi-horizon information-gap decision theory model instead of assuming a probability distribution function or confidence interval for uncertain parameters, and ensure that a predefined minimum allowable benefit is achieved. In [17], deterministic price based unit commitment model that takes into account balance and security constraints of VPP participating in the joint market of the energy and spinning reserve service has been proposed. Using technical and economic dispatch model, technical and economic dispatch problems has been established by utilizing wind power plants, hydroelectric power plants, and on-site solar power in [18].

Reference [19] has proposed an optimal power dispatch strategy to minimize power purchase costs and maximize power sales benefits when VPP including interruptible loads, energy storage systems, and battery switch stations participate in a unified electricity market combining day-ahead and real-time trading. A short-term operational planning framework for a VPP has been proposed in [20]. The stochastic bidding model is proposed in the first stage, that utilizes the Monte-Carlo method to deal with uncertainty, and in the second stage the real-time control operation is optimized using the model predictive control methodology.

Reference [21] have proposed a two-stage stochastic offering model for the maximum profit of VPP participating in DAM and RTM, and evaluated the model for wind power plants, conventional power plants, and pumped hydro storage plants. In [22], DERs and VPP conduct internal transactions to maximize market participation profits of VPP and the surplus profit are distributed to each DER using game theory-based methods. In [23], an interactive dispatch model of multi-VPP based on the DR and game theory has been proposed. Reference [24] has been addressed an architecture and a strategy for cost minimization of a VPP participating in demand side management programs. In [25], a deep reinforcement learning algorithm for an optimal online economic dispatch strategy for VPP with a design of edge-computing based three-layer system architecture has been proposed.

Authors in [26] have proposed a coordinated offering and bidding mechanism for a hybrid power plant containing a concentrated solar power plant, a wind farm, a compressed air energy storage, and a demand response provider by establishing a bi-objective optimization model for constant value-at-risk (CVaR) based strategy as well as considering of participation in the intraday market. In [27], using CVaR approach a multi-objective optimization problem in a joint market of energy and spinning reserve has been proposed, where the demand side resources participate in reserve provision. The problem is solved in a risk-averse probabilistic framework considering various normal operation uncertainties and N-1 contingencies. In [28], authors have proposed a multi-objective bidding strategy of VPP including wind-thermal-photovoltaic system participating in the energy and spinning reserve market to maximize profit and minimize emission. Authors in [29] have proposed a three-stage stochastic multi-objective model for the purpose of profit maximization and emission minimization of wind-thermal-energy storage resources participating in energy, spinning reserve, and imbalance market. To deal with multi-objective problem, lexicographic optimization and hybrid augmented-weighted epsilon constraint method are implemented. In [30], a coordinated operation strategy for hybrid power plant containing wind, photovoltaic, battery energy storage, CAES, and thermal units has been presented considering uncertainty of intraday demand response exchange market and risk measuring indices corresponding to CVaR and deviation of the objective function.

In most of the literature, only individual resources have been addressed as participating in a VPP, and participation of aggregation resources has rarely been considered except for [10]–[12]. As mentioned in [6], a distributed energy resource aggregation (DERA) such as MGs can also participate in VPP. The DERA may have a dedicated management system, so in terms of distributed control, direct interaction between the VPP and the DERA's individual resources is inefficient. Thus, the VPP may establish a bidding strategy for the electricity market in forms of interaction with each DERA.

In addition, most of the literature have not addressed the issue of ownership participating in VPP in detail. In practical circumstances, a VPP operator and owners of each resource may be different and will trade energy and services with each other through specific contracts. Thus, it is necessary to deal with control authority or profit distribution issues when different resources participate in the VPP. Profit distribution according to ownership has been covered in [9] and [22], but these studies have not considered participation of aggregation resources such as MGs in the VPP.

Penalties should also be considered if resources with different ownerships do not respond properly to VPP's real-time dispatch signal. In practical, there may be a case in which the VPP resource does not properly respond to the DAM bid in real time due to problems such as forecast errors or system failures. It is unreasonable for VPP to equally compensate for resources that properly responded to the real-time dispatch signal of the VPP and the resource that did not respond to it. However, most studies have not properly addressed this issue.

In this paper, it is proposed that an optimal operation strategy of the VPP considering uncertainties of real-time dispatch response of the DERA in order to achieve maximum profit of the VPP and the DERA. The degree of responses of the DERA's DAM bid in a real-time environment is assessed daily by the VPP. According to results of the assessment, the VPP determines internal prices of the DERA, and the DERA adjusts its bid range. By repeating these processes, the optimal operational strategy can be established. A pricing function of the DERA is set as a cost that the VPP pays to the DERA. Then, parameters of the pricing function are continuously updated according to the responses of the DERA's DAM bid in the real-time environment to impose penalties to the DERA. Through the iterative process, coordination between the VPP and the DERA can be established and as a result the responsiveness of the real-time dispatch responses of the DERA is improved.

The main contributions of this paper are summarized as follows:

- Establish a profit or cost distribution methodology of DERAs in a VPP to manage real-time uncertainty by a proposed pricing function parameter updating process.
- The DERA can take responsibility on its own uncertainty by a proposed coordination process that the VPP transmits evaluation results of the DERA's real-time operation, and the DERA adjusts its energy reserve for the next day.
- The DERA's capability to manage real-time uncertainty can be increased.

The remainder of this paper is organized as follows. Chapter II describes the problem. Chapter III deals with mathematical models, including a DAM bidding model, DERA pricing function, and an RTM bidding model. In Chapter IV, a simulation based on certain scenarios conducted to verify the proposed model is described. Chapter V presents some concluding remarks and areas of future study.

II. PROBLEM DESCRIPTION

A. DER TYPE AND PARTICIPATION

In this study, the proposed method is modeled for photovoltaic (PV) systems, ESS, MG, electric vehicle aggregation (EVA), and demand response aggregation (DRA). With regard to PV systems, it is assumed that if the owners are the same, it is treated as a single PV system regardless of whether it is a single PV system connected to one transformer or a large-scale PV plant and is always controlled through maximum power point tracking for maximum profit in the power market. That is, the PV generation is not curtailed. Thus, PV generation is treated as a forecasted value. PV generation forecasts are not discussed herein, because they are outside the scope of this paper. The ESS in this paper indicates BESS, which is currently the most widely deployed version. For the VPP to participate in the power market, ESSs are essential because they have a fast response time and can act as both load and power generation. Thus, it is assumed that the VPP operator has the authority to control the ESSs through dedicated contracts between the VPP operator and the ESS owners. DERAs, such as MG, EVA, and DRA, are all in the form of an aggregation of individual resources. Individual resources belonging to DERAs may have different owners, but it is common for DERAs to have a dedicated management system. In the case of MG, the MG energy management system is responsible for cost-minimization operations by maximizing the self-consumption and islanding operations to provide resiliency even in the case of a power system fault [31]. EVA can be regarded as an EV charging station, and the charging station management system can provide services to each EV through functions such as charge/discharge metering, time of use based minimum cost charge/discharge, and participation in the power market through a vehicle-to-grid system [32]. DRA also provides a load curtailment capacity by interacting with external systems through contracts with individual load resources.

DERA management systems are characterized by scheduling functions, individual resource control functions, and external system interaction functions. If VPP directly interacts with individual resources inside the DERAs, operational inefficiencies owing to redundant infrastructure construction and computational complexity will be extremely large and may also not benefit individual resources because it directly leads to a decline in VPP profits. Therefore, it is efficient for the VPP to interact only with DERA operators to transact energy and services with each other.

Each DERA submits its own bidding schedule before the VPP implements the electricity market bidding schedule. In this paper, it is assumed that MGs have ESSs for efficient self-consumption, and thus it is possible to adjust their own bidding range. In addition, EVAs and DRAs do not have dedicated ESSs, thus they are not able to efficiently respond to uncertainties. The purpose of this assumption is to ensure that the uncertainties that may occur in a real-time environment can be addressed by the dispatchable resources, and that the profit distribution of each participant is determined according to their responsiveness, thereby inducing active participation of the participants.

B. ELECTRIC POWER MARKET

In this paper, the power market in which a VPP participates is assumed to be an energy market composed of DAM and RTM. The Korean power market is a cost-based pool and only has DAM, in which an operation schedule that reflects power system constraints is determined after the market price is determined through a non-constrained problem that does not reflect power system constraints such as transmission and heat constraints. The difference between the power generation plan and the actual output of the generators is then compensated with the constrained settlement. However, to solve the problem of accepting renewable energy at the market level while reflecting the actual conditions of the power supply and demand as well as the power system, Korea is currently pursuing a reform of the power market. First, through the reform of the energy settlement, the generation scheduling will be unified, and the compensation for flexible resources will be systematized through the reform of the auxiliary service settlement. Finally, DAM and RTM with price bidding are expected to be opened in 2024. The Korean power market is based on the North American power market. In North America DAM, RTO/ISO receives bidding data with economic and technical characteristics from generators to optimize the market in a centralized fashion. During an RTM operation, the RTOs/ISOs are responsible for the balance of supply and demand, and deviations from the DAM generation schedule are settled at RTM prices. Therefore, to utilize the human and physical infrastructure already deployed in Korea, it is expected that the direction of the reform of the Korean power market will also be based on the North American model.

The electric power market prices applied to the VPP in this study consist of wholesale market sales/purchase prices and retail market sales/purchase prices. The wholesale market sales price is generally the price at which the dispatchable generator sells the energy required to operate the power system; in this case, the price when the VPP energy is sold to the wholesale market. The wholesale market purchase price is the price at which the load serving entity (LSE) purchases power from the wholesale market to supply power to their load. The retail market sales price is the price of selling surplus energy of behind-the-meter ESS and PV to LSE, and the retail market purchase price is the price applied to consume the load. For purchases, the LSE profits depend on the difference between the wholesale market purchase price that the LSEs pay to the wholesale market and the retail market purchase price that the load pays to the LSEs. In general, the retail market purchase price is generally higher than the wholesale market purchase price. For sales, it is reasonable that the wholesale market sales price, which is the source of profit for the dispatchable generators, is higher than the retail market sales price at which the BTM resources sell surplus energy to the LSEs. In addition, for the same product, the price purchased in the market is higher than the price sold in the market. Therefore, in this study, it is assumed that the energy prices have an order of the retail market purchase price, wholesale market purchase price, wholesale market sales price, and retail market sales price. Then, from the perspective of the VPP, minimizing the quantity of purchase is more advantageous than maximizing the profit from selling the surplus energy. In other words, the VPP will operate in the direction of maximizing self-consumption. From the perspective of DERs inside the VPP, it is more profitable to sell the surplus energy to the wholesale market than to sell it to the retail market, which guarantees the feasibility of the participation of the DER in the VPP.

C. DER COMMUNICATION

It is assumed that communication latency between the VPP and each participant is zero or negligible. A VPP may have a cloud platform-based management system owing to its geographical dispersion characteristics. Wired and/or wireless communication such as TCP/IP, LTE, and Wi-Fi can be used between the VPP and each participant [6]. Communication methods may have latency, but a latency of a few seconds, which can occur in practice, is not expected to have a significant impact on the application of the strategy proposed in this paper. It is therefore assumed that the interaction between the VPP and the participants, by which the VPP receives the real-time monitoring status of each participant and transmits dispatch signals, is immediately applied.

III. MATHEMATICAL MODELING

Mathematical modeling of the problem discussed in Chapter II is described in this chapter. The purpose of this study is to distribute profit or cost to each DERA according to the real-time responsiveness with respect to their DAM schedule so that they take responsibility for handling the real-time uncertainty on their own. Thus, the mathematical model includes a DAM bidding, DERA pricing function, and an RTM bidding as well as each DERA's bidding.

The pricing function consists of a quadratic equation, and the whole problem becomes mixed-integer quadratic programming. The objective function result that does not include the pricing function is the VPP's maximum profit. The result is the optimal solution that the VPP can obtain. In other words, the VPP's maximum profit is not guaranteed outside

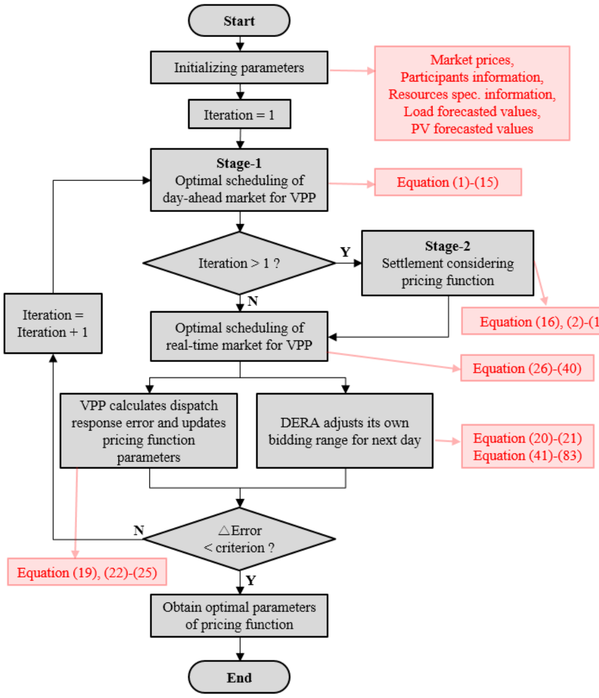

FIGURE 2. **Total flow chart for solving two-stage problem.**

this solution. Because the purpose of the pricing function is for the VPP to price according to participants' dispatch result and allocate profits to them, if the pricing function is included in an entire problem, the solution result may be lower due to the quadratic equation of the pricing function. Therefore, the entire problem is divided into two stages: Stage 1, which determines bid quantity for the VPP's maximum profit and whether to purchase or sell, and Stage 2, which determines the DERA's internal price by the pricing function for a predetermined energy bid in Stage 1. In this case, Stage 1 becomes a mixed-integer linear programming problem, and Stage 2 becomes a quadratic programming problem. Fig. 2 presents a flow chart for solving these two-stage problems. First, after the initial setting, Stage 1 is applied to maximize the VPP profit in DAM, and Stage 2 is conducted, except during the initial iteration, to evaluate the DERA performance once a day. After that, the real-time market operation every 5 minutes over 24 hours is performed to fully satisfy the DAM schedule, and the parameters for evaluating the real-time operation result are updated. DAM bidding is conducted again for the next day.

As proposed in this paper, however, it is necessary to determine whether difference in error along the iteration falls below a tolerance in the simulation to verify the validity of the methodology for securing additional reserve energy in DAM to reduce the real-time fluctuation of DERA on its own. When a VPP is actually in commercial operation, each parameter is determined through a daily performance evaluation process. Because one iteration corresponds to one day, it may take time to identify that difference in error converges on an actual operation. However, if a decrease trend of difference in error within a certain level is identified with a simulation, it is expected that it will not be needed to check whether difference in error converges every time on the actual operation.

A. DAY-AHEAD MARKET BIDDING

1) STAGE 1: BIDDING MODEL FOR MAXIMIZING DAY-AHEAD MARKET PROFIT OF VPP

An objective function for the maximum profit of the VPP when bidding for DAM is as follows:

$$Max \sum_{t=1}^{T} \left[\pi_{DA}^{s}(t) \, P_{DAbid}^{VPP,s}(t) - \pi_{DA}^{b}(t) \, P_{DAbid}^{VPP,b}(t) \right] \quad (1)$$

The constraints are as follows:

$$P_{DAbid,i}^{c}(t) = \begin{cases} P_{DAbid,i}^{PV}(t) - P_{DAload,i}^{PV}(t), & \forall c \in \widehat{PV} \\ P_{DAbid,i}^{ESS}(t) - P_{DAload,i}^{ESS}(t), & \forall c \in \widehat{ESS} \\ P_{DAsche,i}^{EVA}(t) + P_{DAbid,i}^{EVA}(t), & \forall c \in \widehat{EVA} \\ P_{DAsche,i}^{DRA}(t) + P_{DAbid,i}^{DRA}(t), & \forall c \in \widehat{DRA} \\ P_{DAsche,i}^{MG}(t) + P_{DAbid,i}^{MG}(t), & \forall c \in \widehat{MG} \end{cases} \quad (2)$$

$$P_{DAbid}^{VPP,s}(t) - P_{DAbid}^{VPP,b}(t) = \sum_{i=1}^{N} P_{DAbid,i}^{c}(t) \quad (3)$$

$$SOC_i^c(t+1) = SOC_i^c(t) + \frac{\eta_i^c P_{DAbid,i}^{c,ch}(t) - \left(1/\eta_i^c\right) P_{DAbid,i}^{c,dch}(t)}{Cap_i^c} \Delta t, \ \forall c \in \widehat{ESS} \quad (4)$$

$$SOC_i^c(0) = SOC_i^{c,ini} \quad (5)$$

$$SOC_i^c(T) = SOC_i^{c,end} \quad (6)$$

$$SOC_i^{c,lb} \le SOC_i^c(t) \le SOC_i^{c,ub} \quad (7)$$

$$\mu_{DA,i}^{c,ch}(t) + \mu_{DA,i}^{c,dch}(t) \le 1 \quad |\mu_{DA,i}^{c,dch}(t), \mu_{DA,i}^{c,ch}(t) \in \{0,1\}, \quad \forall c \in \widehat{ESS} \quad (8)$$

$$0 \le P_{DAbid,i}^{c,ch}(t) \le P_{DAbid,i}^{c,ch,max}(t) \, \mu_{DA,i}^{c,ch}(t), \ \forall c \in \widehat{ESS} \quad (9)$$

$$0 \le P_{DAbid,i}^{c,dch}(t) \le P_{DAbid,i}^{c,dch,max}(t) \, \mu_{DA,i}^{c,dch}(t), \quad \forall c \in \widehat{ESS} \quad (10)$$

$$P_{DAbid,i}^{c}(t) = P_{DAbid,i}^{c,dch}(t) - P_{DAbid,i}^{c,ch}(t), \ \forall c \in \widehat{ESS} \quad (11)$$

$$0 \le P_{DAbid}^{VPP,b}(t) \le P_{DAbid}^{VPP,b,max}(t) \, \mu_{DA}^{b}(t) \quad (12)$$

$$0 \le P_{DAbid}^{VPP,s}(t) \le P_{DAbid}^{VPP,s,max}(t)\,\mu_{DA}^{s}(t) \quad (13)$$

$$\mu_{DA}^{s}(t) + \mu_{DA}^{b}(t) \le 1 | \mu_{DA}^{s}(t),\, \mu_{DA}^{b}(t) \in \{0,1\} \quad (14)$$

$$P_{DAbid,i}^{c,min}(t) \le P_{DAbid,i}^{c}(t) \le P_{DAbid,i}^{c,max}(t) \quad (15)$$

Equation (2) is a constraint on each DER or DERA bidding on the VPP. As mentioned earlier, the PV generation is treated as forecast values, and the ESS is directly controlled by the VPP operator to manage fluctuations. The DERA submits its bidding plan to the VPP in the form of adding reserves to its plan if needed. Equation (3) means that when the bid quantity of each DER or the DERA is summed, the total quantity of bidding in the power market of the VPP is obtained. Equations (4)–(7) are constraints on the ESS SOC. Equation (4) represents the SOC change over time, (5) and (6) represents the initial/end conditions of the SOC, and (7) represents its upper/lower limits. Equations (8)-(10) means that the ESS cannot be allowed to charge and discharge at the same time while satisfying the upper limits. Internal bid quantity of the ESS is calculated by subtracting charge energy from discharge energy, as presented in equation (11).

Equations (12)–(14) are the VPP purchase/sell bidding restrictions. They are the constraints such that the VPP cannot be allowed to purchase and sell at the same time while satisfying the upper limits. Equation (15) is the upper and lower limit of the participant bids. Because the DERA calculates its energy reserves independently, the upper and lower limits refer to the range of bidding submitted by the DER to the VPP.

2) STAGE 2: BIDDING MODEL CONSIDERING DER PRICING FUNCTION

In Stage 2, profit sharing is conducted by considering the results of Stage 1 and the DERA pricing function. The objective function of Stage 2 is a form that considers the objective function of Stage 1 with the pricing function and is expressed as follows:

$$max \sum_{t=1}^{T}\left[\pi_{DA}^{s}(t)\,P_{DAbid}^{VPP,s*}(t) - \pi_{DA}^{b}(t)\,P_{DAbid}^{VPP,b*}(t) - \sum_{i=1}^{N} C_i^c(t)\right] \quad (16)$$

The constraints are the same as for Stage 1 except for (12)–(14) because it is assumed that sales or purchase has been determined in Stage 1. A superscript '*' in equation (16) means the bid quantity already determined in Stage 1.

3) DERA PRICING FUNCTION

Here, the pricing function in the form of a quadratic equation for determining the internal price of each DERA is formulated. In general, the cost function of the generator used in the power dispatch schedule required for the operation of the entire power system is expressed in the form of a quadratic equation that opens upward, and the market price is determined at the point where the marginal cost of all generators becomes the same as a result of the economic dispatch calculation. In this study, using this principle, we assumed that the pricing function of each DERA also follows the quadratic equation form and tries to find the marginal price:

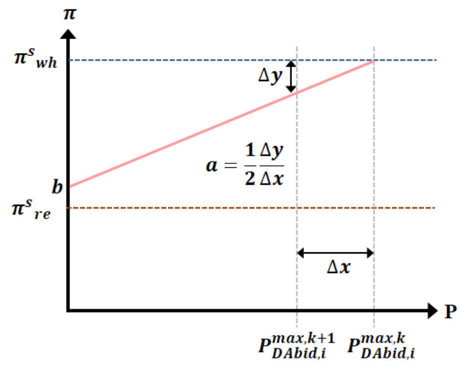

FIGURE 3. Determining each coefficient (selling case).

$$C_i^c(t) = a_i^c(t)\,P_{DAbid,i}^{c}(t)^2 + b_i^c(t)\,P_{DAbid,i}^{c}(t) \quad (17)$$

$$C_i^{c\prime}(t) = 2a_i^c(t)\,P_{DAbid,i}^{c}(t) + b_i^c(t) \quad (18)$$

The pricing function coefficients of each DERA, $a_i^c(t)$ and $b_i^c(t)$, are repeatedly updated according to the predefined criterion. Equation (18) is a derivative of (17); thus, it is a linear equation representing the marginal price. The price applied to each DERA is the marginal price, which is updated repeatedly depending on $a_i^c(t)$ and $b_i^c(t)$. Fig. 3 shows the marginal price curve and how each coefficient is determined for the sales time period. The purchase time period has a negative power; however, because the mechanism is the same as that of the sale time period, only the method of the sale time period is described here.

For the sales time period, the maximum internal price of the DERA is the wholesale market sales price, and the minimum internal price is the retail market sales price. The internal price applied to the DERA is determined within this price range. The coefficients for the marginal price function of (18) represent the slope and y-intercept, respectively. First, the slope for the k+1-th day is determined as follows:

$$a_i^c(t) = \frac{1}{2}\frac{\Delta y}{\Delta x} \quad (19)$$

If the DAM schedule is not satisfied owing to uncertainties such as a forecast error or failure in real-time circumstances, the DERA adjusts the DAM bid quantity for the next day. Because the resources held by the DERA have already been determined in an actual environment, it is impractical to reinforce additional DER equipment to cope with real-time uncertainty. In this study, it is assumed that by narrowing the SOC range of the ESS held by the DERA, the range of energy reserves for the DAM bidding is widened, and the additional energy generated by the narrowed SOC range is assumed to cope with the real-time uncertainty. If the amount of generated energy is as insufficient as ΔE_{down}, and uncertainty can be properly responded to in a real-time situation over a day, the lower SOC limit needs to be increased to a certain extent. In addition, if the amount of energy generated exceeded ΔE_{up}, the upper limit of SOC must be lowered:

$$SOC_i^{c,ub} = SOC_i^{c,ub} - \varepsilon \Delta E_{down} \tag{20}$$

$$SOC_i^{c,lb} = SOC_i^{c,lb} + \varepsilon \Delta E_{up} \tag{21}$$

Equations (20) and (21) indicate that the DERA has an additional energy reserve for charge/discharge. Coefficient ε is the step size for adjusting the SOC upper/lower limits. The DERA reflects the adjusted SOC upper/lower limits in its DAM bidding on the next day.

For any DERAs, supposing that the maximum bid quantity for each k-th day is $P_{DAbid,i}^{c,max,k}(t)$ and that the maximum bid quantity for the k+1-th day that reflects the adjusted SOC on the next day is $P_{DAbid,i}^{c,max,k+1}(t)$, because it cannot respond to uncertainty, the DERA will bid for DAM with the adjusted upper/lower limit of the SOC. This means that less energy is available than on the previous day, and Δx can be calculated as follows:

$$\Delta x(t) = P_{DAbid,i}^{c,max,k}(t) - P_{DAbid,i}^{c,max,k+1}(t) \tag{22}$$

Because the size of Δy will be determined between the wholesale market sales price and the retail market sales price, Δy will be a ratio multiplied by the difference between the two prices:

$$\Delta y(t) = \gamma_i^c(t) \cdot (\pi_{wh}^{s,k+1}(t) - \pi_{re}^{s,k+1}(t)) \tag{23}$$

The larger the error rate is, the larger the ratio $\gamma_i^c(t)$. This means that the larger the error rate is, the lower the DERA internal price according to the marginal price curve:

$$\gamma_i^c(t) = \frac{\left|P_{DAbid,i}^{c,k}(t) - \sum P_{RTbid,i}^{c,k}(t)/12\right|}{P_{DAbid,i}^{c,k}(t)} \tag{24}$$

In equation (24), the second term of the numerator on the right-hand side means the 1-hour average of real-time bidding values. This values are used to coherently calculate $\gamma_i^c(t)$ from 1-hour based day-ahead values and 5-minutes based real-time values.

The coefficient $b_i^c(t)$ for the k+1-th day can be obtained using Equation (18):

$$b_i^c(t) = \pi_{wh}^s(t) - 2a_i^c(t) P_{DAbid,i}^{c,max,k+1}(t) \tag{25}$$

Internal price $C_i^{c\prime}$ in equation (18) does not directly affect DERA's real-time responsiveness to manage uncertainty. In actual VPP operation, the DERA will adjust additional reserve indirectly through $C_i^{c\prime}$, and directly through ΔE_{up} or ΔE_{down} determined by the VPP operator as a result of real-time response. That is, $C_i^{c\prime}$ has meaning of a sort of performance score that indirectly informs the DERA's adjustment results. If the DERA determines that its internal price is acceptable within an expected range, then no further reserve adjustment will be made. Otherwise, the DERA will continue to adjust the reserve based on the parameter ε in equation (20) and (21).

B. REAL-TIME MARKET BIDDING

The RTM bidding model is formulated based on the DAM bidding model. The purpose of RTM bidding is to satisfy the DAM schedule as much as possible. According to [33], the current RTO/ISO real-time market settlement takes place every 5 min. In this paper, therefore, the time interval of real-time market operation is basically 5 min, but it can be flexibly applied according to the policy of any market operators.

The objective function is as follows:

$$max \sum_{t=1}^{T} \left[\pi_{RT}^s(t) P_{RTbid}^{VPP,s}(t) - \pi_{RT}^b(t) P_{RTbid}^{VPP,b}(t)\right] \tag{26}$$

The constraints are as follows:

$$P_{DAbid}^{VPP,s*}(t) - P_{DAbid}^{VPP,b*}(t) + P_{RTbid}^{VPP,s}(t) - P_{RTbid}^{VPP,b}(t) = \sum_{i=1}^{N} \left(P_{DAbid,i}^{c*} + P_{RTbid,i}^{c}(t)\right) \tag{27}$$

$$SOC_i^c(t+1) = SOC_i^c(t) + \frac{P_{DAbid,i}^{c*}(t)}{Cap_i^c} + \frac{\eta_i^c P_{RTbid,i}^{c,ch}(t) - (1/\eta_i^c) P_{RTbid,i}^{c,dch}(t)}{Cap_i^c}\Delta t, \ \forall c \in \widehat{ESS} \tag{28}$$

$$0 \le P_{RTbid}^{VPP,b}(t) \le P_{RTbid}^{VPP,b,max}(t)\,\mu_{RT}^b(t) \tag{29}$$

$$0 \le P_{RTbid}^{VPP,s}(t) \le P_{RTbid}^{VPP,s,max}(t)\,\mu_{RT}^s(t) \tag{30}$$

$$\mu_{RT}^s(t) + \mu_{RT}^b(t) \le 1 | \mu_{RT}^s(t), \mu_{RT}^b(t) \in \{0,1\} \tag{31}$$

$$SOC_i^c(0) = SOC_i^{c,ini} \tag{32}$$

$$SOC_i^c(T) = SOC_i^{c,end} \tag{33}$$

$$SOC_i^{c,lb} \le SOC_i^c(t) \le SOC_i^{c,ub} \tag{34}$$

$$\mu_{RT,i}^{c,ch}(t) + \mu_{RT,i}^{c,dch}(t) \le 1 \ |\mu_{RT,i}^{c,ch}(t), \mu_{RT,i}^{c,dch}(t) \in \{0,1\} \tag{35}$$

$$0 \le P_{RTbid,i}^{c,ch}(t) \le P_{RTbid,i}^{c,ch,max}(t)\,\mu_{RT,i}^{c,ch}(t), \ \forall c \in \widehat{ESS} \tag{36}$$

$$0 \le P_{RTbid,i}^{c,dch}(t) \le P_{RTbid,i}^{c,dch,max}(t)\,\mu_{RT,i}^{c,dch}(t), \ \forall c \in \widehat{ESS} \tag{37}$$

$$P_{RTbid,i}^{c}(t) = P_{RTbid,i}^{c,dch}(t) - P_{RTbid,i}^{c,ch}(t) \ | \ \forall c \in \widehat{ESS} \tag{38}$$

$$P_{RTbid,i}^{c,min}(t) \le P_{RTbid,i}^{c}(t) \le P_{RTbid}^{c,max}(t) \tag{39}$$

$$\sum_{i=1}^{N} P_{bid,i}^{MG,RT}(t) = E_{MG} \tag{40}$$

A superscript '*' in (27), (28) means the bid quantity already determined in the DAM.

C. DERA BIDDING

The DERAs in this paper include a MG, an EVA, and a DRA. Inside the MG, ESSs and PVs may exist for resiliency and self-consumption, and their self-scheduling results are supposed to be submitted to the VPP. The EVA randomly set the entry/exit time and entry SOCs of each EV, whereas exit SOCs are received from the EVs. It is assumed that the DRA have a small-scale PV and submit a DAM bid energy to the VPP considering the hourly based flexible load response.

1) MG BIDDING FORMULATION

The MG in this paper is assumed to have members of one PV and ESS. The objective function is as follows:

$$\min \sum_{t=1}^{T} \left(\pi_{re}^{b}(t) P_{b}^{MG}(t) - \pi_{re}^{s}(t) P_{s}^{MG}(t) \right) \tag{41}$$

where P_b^{MG}/P_s^{MG} is the MG's purchase/sales energy at a point of common coupling.

The constraints are as follows.

Balance constraint:

$$P_b^{MG}(t) - P_s^{MG}(t) + P_{dch}^{ESS}(t) - P_{ch}^{ESS}(t) = P_{load}(t) - P_{PV}(t) \tag{42}$$

where $P_{dch}^{ESS}/P_{ch}^{ESS}$ are discharge/charge energy of the ESS respectively, P_{load} and P_{PV} means forecasted values of the MG load and PV generation.

ESS SOC constraint:

$$SOC(t+1) = SOC(t) + \frac{\eta_{ESS} P_{ch}^{ESS}(t) - (1/\eta_{ESS}) P_{dch}^{ESS}(t)}{Cap_{ESS}} \Delta t \tag{43}$$

where $SOC(t)$ is SOC of MG ESS at time t, η_{ESS} is an ESS efficiency, and Cap_{ESS} is a rated capacity of the ESS.

Constraints on avoiding simultaneous purchase/sales, and charging/discharging:

$$0 \le P_b^{MG}(t) \le \mu_b^{MG}(t) P_{b,max}^{MG} \tag{44}$$

$$0 \le P_s^{MG}(t) \le \mu_s^{MG}(t) P_{s,max}^{MG} \tag{45}$$

$$\mu_b^{MG}(t) + \mu_s^{MG}(t) \le 1 | \mu_b^{MG}(t), \mu_s^{MG}(t) \in \{0,1\} \tag{46}$$

$$0 \le P_{dch}^{ESS}(t) \le \mu_{dch}^{ESS}(t) P_{dch,max}^{ESS} \tag{47}$$

$$0 \le P_{ch}^{ESS}(t) \le \mu_{ch}^{ESS}(t) P_{ch,max}^{ESS} \tag{48}$$

$$\mu_{dch}^{ESS}(t) + \mu_{ch}^{ESS}(t) \le 1 | \mu_{dch}^{ESS}(t), \mu_{ch}^{ESS}(t) \in \{0,1\} \tag{49}$$

where μ_b^{MG}/μ_s^{MG} are binary variable to indicate purchase/sales energy, $P_{b,max}^{MG}/P_{s,max}^{MG}$ are upper bounds of purchase/sales energy, $\mu_{dch}^{ESS}/\mu_{ch}^{ESS}$ are binary variable to indicate ESS discharging/charging status, and $P_{dch,max}^{ESS}/P_{ch,max}^{ESS}$ mean ESS discharge/charge energy upper bounds.

Lower/upper bounds constraints:

$$SOC^{MG,lb} \le SOC(t) \le SOC^{MG,ub} \tag{50}$$

where $SOC^{MG,ub}$, $SOC^{MG,lb}$ corresponds to equation (20), (21) respectively so that the MG's reserve adjusts through iteration process.

Constraint on the initial SOC condition:

$$SOC_{init} = SOC_{end} = 0.5 \tag{51}$$

The MG calculates the internal bidding energy according to followed procedure.

(a) At first, the MG calculates its net demand:

$$P_{netd}(t) = P_{load}(t) - P_{PV}(t) \tag{52}$$

(b) The MG solves scheduling model above.

As a result, MG decides on its components' schedule and energy to purchase ($P_b^{MG}(t)$) from the grid, or sell ($P_s^{MG}(t)$) into the grid.

Positive $P_{netd}(t)$ mean that additional energy is supplied from the grid. At this time, if $P_b^{MG}(t)$ is greater than $P_{netd}(t)$, it means that some components are acting as an additional load. In this case, the range of purchase bids of the MG is as follows:

$$P_{netd}(t) \le P_{DAbid}^{MG}(t) \le P_b^{MG}(t)$$

On the contrary, if $P_b^{MG}(t)$ is smaller than $P_{netd}(t)$, the range of purchase bids of the MG is as follows:

$$P_b^{MG}(t) \le P_{DAbid}^{MG}(t) \le P_{netd}(t)$$

Negative $P_{netd}(t)$ mean that excess energy is injected to the grid. At this time, if the value of $P_s^{MG}(t)$ is larger than the absolute value of $P_{netd}(t)$, it can be considered that distributed resources additionally supply and sell energy.

Therefore, the range of the MG's sales bidding is as follows:

$$-P_s^{MG}(t) \le P_{DAbid}^{MG}(t) \le P_{netd}(t)$$

On the contrary, if the value of $P_s^{MG}(t)$ is smaller than the absolute value of $P_{netd}(t)$, it means that distributed resources such as ESS are charging. Therefore, the sales bidding range is:

$$P_{netd}(t) \le P_{DAbid}^{MG}(t) \le -P_s^{MG}(t)$$

2) EVA BIDDING FORMULATION

The EVA in this paper is assumed to have a total of N numbers of EV resources. The objective function is as follows:

$$min \sum_{t=1}^{T} (\pi_{re}^{b}(t) P_b^{EVA}(t) - \pi_{re}^{s}(t) P_s^{EVA}(t)) \tag{53}$$

where P_b^{EVA}/P_s^{EVA} are purchase/sales energy of the EVA.

The constraints are as follows.

Balance constraints:

$$P_s^{EVA}(t) - P_b^{EVA}(t) = \sum_{j=1}^{N} \left(P_{dch,j}^{EV}(t) - P_{ch,j}^{EV}(t)\right) \quad (54)$$

where $P_{dch,j}^{EV}/P_{ch,j}^{EV}$ are discharging/charging energy of j-th EV.

Constraints on EV battery SOC for j-th EV:

$$SOC_j^{EV}(t+1) = SOC_j^{EV}(t) + \frac{\eta_{EV} P_{ch,j}^{EV}(t) - (1/\eta_{EV}) P_{dch}^{EV}(t)}{Cap_{EV,j}} \Delta t \quad (55)$$

$$SOC_j^{EV}(1) = SOC_{init,j}^{EV}(t) \quad (56)$$

$$SOC_j^{EV}(T) = SOC_{end,j}^{EV}(t) \quad (57)$$

where $SOC_j^{EV}(t)$ is SOC of j-th EV at time t, η_{EV} is an EV efficiency, and $Cap_{EV,j}$ is a rated capacity of j-th EV.

Constraints on avoiding simultaneous charging and discharging:

$$\mu_{dch,j}^{EV}(t) + \mu_{ch,j}^{EV}(t) \leq 1 | \mu_{dch,j}^{EV}(t), \mu_{ch,j}^{EV}(t) \in \{0,1\} \quad (58)$$

$$0 \leq P_{dch,j}^{EV}(t) \leq \mu_{dch,j}^{EV}(t) P_{rate,j}^{EV} \quad (59)$$

$$0 \leq P_{ch,j}^{EV}(t) \leq \mu_{ch,j}^{EV}(t) P_{rate,j}^{EV} \quad (60)$$

where $\mu_{dch,j}^{EV}/\mu_{ch,j}^{EV}$ are binary variable to present discharging/charging status of j-th EV, and $P_{rate,j}^{EV}$ is a rated power of j-th EV.

Constraints on avoiding simultaneous purchase and sales:

$$\mu_b^{EVA}(t) + \mu_s^{EVA}(t) \leq 1 | \mu_b^{EVA}(t), \mu_s^{EVA}(t) \in \{0,1\} \quad (61)$$

$$0 \leq P_b^{EVA}(t) \leq \mu_b^{EVA}(t) P_{b,max}^{EVA} \quad (62)$$

$$0 \leq P_s^{EVA}(t) \leq \mu_s^{EVA}(t) P_{s,max}^{EVA} \quad (63)$$

where μ_b^{EVA}/μ_s^{EVA} are binary variables indicating purchase/sales status and $P_{b,max}^{EVA}/P_{s,max}^{EVA}$ are purchase/sales energy of the EVA.

Constraints on upper and lower bounds of EVA energy:

$$0 \leq P_{dch,j}^{EV}(t) \leq b_j^{op}(t) P_{rate,j}^{EV} \quad (64)$$

$$0 \leq P_{ch,j}^{EV}(t) \leq b_j^{op}(t) P_{rate,j}^{EV} \quad (65)$$

where $b_j^{op}(t)$ is an operation time index that indicates whether the EVs are ready for charge (1: connected to the charger, 0: not connected to the charger, or not be in the charging station).

EV SOC constraints:

$$SOC_{min,j} \leq SOC_j^{EV}(t) \leq SOC_{max,j} \quad (66)$$

$$0 \leq \mu_{dch}^{EV}(t) \leq b_j^{op}(t) \quad (67)$$

$$0 \leq \mu_{ch}^{EV}(t) \leq b_j^{op}(t) \quad (68)$$

The EVA solves the schedule model so that it can decide the bid energy P_b^{EVA} and P_s^{EVA}. The EVA is assumed not to have internal resources that can be dispatched while the MG decides the bid energy with reserve for adjustment.

3) DRA BIDDING FORMULATION

The DRA in this paper is assumed to have a total of M number of DR resources, where each DR resource have both non-flexible loads and flexible loads. Flexible loads are adjusted to respond to DR signals. Flexible loads here are assumed to be shiftable loads such that if the loads are reduced at some times, then the loads should be increased at the other times. The objective function is as follows:

$$min \sum_{t=1}^{T} \left(\pi_{re}^{b}(t) P_b^{DRA}(t) - \pi_{re}^{s}(t) P_s^{DRA}(t)\right) \quad (69)$$

where P_b^{DRA}/P_s^{DRA} are purchase/sales energy of the DRA.

The constraints are as follows.

Balance constraints on each DR resource containing avoidance of simultaneous reduction and increase of flexible loads:

$$P_{b,k}^{DR}(t) = P_{load,k}^{DR}(t) + P_{upflex,k}^{DR}(t) - P_{downflex,k}^{DR}(t) - P_{PV,k}^{DR}(t) \quad (70)$$

$$\sum_{k=1}^{M} P_{upflex,k}^{DR}(t) = \sum_{k=1}^{M} P_{downflex,k}^{DR}(t) \quad (71)$$

$$\mu_{upflex,k}^{DR}(t) + \mu_{downflex,k}^{DR}(t) \leq 1 | \mu_{upflex,k}^{DR}(t), \mu_{downflex,k}^{DR}(t) \in \{0,1\} \quad (72)$$

$$0 \leq P_{upflex,k}^{DR}(t) \leq \mu_{upflex,k}^{DR}(t) P_{upflex,k}^{DR,max} \quad (73)$$

$$0 \leq P_{downflex,k}^{DR}(t) \leq \mu_{downflex,k}^{DR}(t) P_{downflex,k}^{DR,max} \quad (74)$$

where $P_{b,k}^{DR}$ is purchase energy, $P_{load,k}^{DR}$ is forecasted non-flexible load amount, $P_{upflex,k}^{DR}/P_{downflex,k}^{DR}$ are up/down energy of flexible load amount, $P_{PV,k}^{DR}$ is forecasted PV generation, $\mu_{upflex,k}^{DR}/\mu_{downflex,k}^{DR}$ are binary variables indicating up/down of flexible load, and $P_{upflex,k}^{DR,max}/P_{downflex,k}^{DR,max}$ are upper bounds. A subscript k means k-th DR resource.

Balance constraints on the DRA containing avoidance of simultaneous purchase and sales:

$$P_s^{DRA}(t) - P_b^{DRA}(t) = \sum_{k=1}^{M} \left(P_{downflex,k}^{DR}(t) - P_{upflex,k}^{DR}(t) - P_{load,k}^{DR}(t) + P_{PV,k}^{DR}(t)\right) \quad (75)$$

$$\mu_b^{DRA}(t) + \mu_s^{DRA}(t) \leq 1 | \mu_b^{DRA}(t), \mu_s^{DRA}(t) \in \{0,1\} \quad (76)$$

$$0 \leq P_b^{DRA}(t) \leq \mu_b^{DRA}(t) P_{b,max}^{DRA} \quad (77)$$

$$0 \leq P_s^{DRA}(t) \leq \mu_s^{DRA}(t) P_{s,max}^{DRA} \quad (78)$$

TABLE 1. Simulation parameters of PV, ESS, and MG.

Parameter	Value	Parameter	Value
PV capacity	400 kW	MG PV capacity	400 kW
ESS capacity	325 kWh	MG ESS capacity	200 kWh
ESS power	250 kW	MG ESS power	200 kW
ESS efficiency	99.54 %	MG ESS efficiency	96.93 %
ESS initial SOC	44.89 %	MG ESS initial SOC	42.93 %
ESS SOC upper/lower limit	81.47 / 23.84 %	MG ESS SOC upper/lower limit	91.77 / 7.16 %

TABLE 2. Simulation parameters of EVA, DRA.

Parameter	Value	Parameter	Value
Num. of EV	7	Num. of DR participants	8
EV charger power	21 kW	DR PV capacity	30 kW
EV capacity	180 kWh	Maximum load of DR	1.3-times
EV charger efficiency	0.98	Minimum load of DR	0.7-times

EV SOC (entry)	EV No.	1	2	3	4
	SOC	0.7229	0.6978	0.7043	0.7596
	EV No.	5	6	7	
	SOC	0.6489	0.2271	0.2341	
EV SOC (exit)	EV No.	1	2	3	4
	SOC	0.5056	0.6687	0.5319	0.5996
	EV No.	5	6	7	
	SOC	0.5070	0.6184	0.6185	

where μ_b^{DRA}/μ_s^{DRA} are binary variables presenting purchase/sales status of the DRA, and $P_{b,max}^{DRA}/P_{s,max}^{DRA}$ are upper bounds of the DRA purchase/sales energy.

Constraints of upper/lower bounds:

$$P_{b,min,k}^{DR} \leq P_{b,k}^{DR}(t) \leq P_{b,max,k}^{DR}(t) \tag{79}$$

$$0 \leq P_{upflex,k}^{DR}(t) \leq a_k(t)\, P_{upflex,k}^{DR,max} \tag{80}$$

$$0 \leq P_{downflex,k}^{DR}(t) \leq a_k(t)\, P_{downflex,k}^{DR,max} \tag{81}$$

$$0 \leq \mu_{upflex,k}^{DR}(t) \leq a_k(t) \tag{82}$$

$$0 \leq \mu_{downflex,k}^{DR}(t) \leq a_k(t) \tag{83}$$

where $P_{b,min,k}^{DR}/P_{b,max,k}^{DR}$ are lower/upper bounds of purchase energy of k-th DR resource, $P_{upflex,k}^{DR,max}/P_{downflex,k}^{DR,max}$ are upper bounds of the flexible load of k-th DR resource, and $a_k(t)$ is an index that indicates whether k-th DR resource can be adjusted at time t (0: non-adjustable, 1: adjustable).

IV. SIMULATION

A. DATA

As mentioned in Section II, the participants in the VPP consist of the PV, the ESS, the MG, the EVA, and the DRA. In the simulation, one of each participant is assumed to participate. The detailed parameters are listed in Tables 1 and 2. The data on the electricity market price, load, and solar irradiation in the Newark area belonging to PJM are used [34]. Through these data, the load curve and PV power generation profile of each participant were derived. For the RTM parameters, a random error-based normal distribution is generated and applied to the DAM forecast to verify the validity of the proposed strategy. The market prices as well as load and PV power of the MG among all the parameters are shown in Fig. 4.

The EVA is assumed to be an EV charging station. The time and SOC for the entry and exit of EVs at the EV charging station are set randomly. Entry and exit times are assumed to occur during rush hours. Because the time and SOC of entry/exit may vary in practical situations, when simulating real-time results, these parameters are randomly changed considering the forecast error.

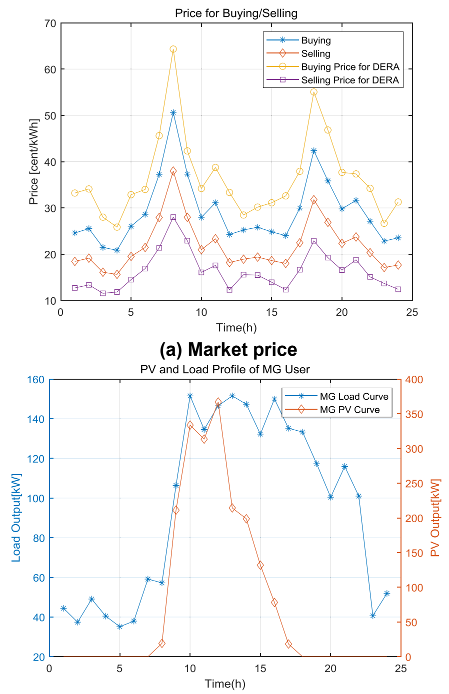

(a) Market price

(b) Load and PV power of the MG

FIGURE 4. Simulation parameters (selected).

B. SIMULATION SCENARIO

The following scenarios in Table 3 are configured to verify the validity of the proposed strategy. Case 1 is the case in which the bid quantity of the DERAs finally determined by the VPP operator is settled at the wholesale market price without adjustment of the bidding strategy of the DERA. Therefore, the pricing function is not used. In other words, because the VPP pays at the wholesale market price for all participants, the VPP's profit is totally distributed to the participants. Case 2 has the same conditions as Case 1 except that the internal price is determined between the wholesale market price and the retail market price based on the calculated error according to the proposed method. Accordingly, participants

TABLE 3. Simulation scenario case.

Item \ Case	Case 1	Case 2	Case 3-1	Case 3-2
Strategy	Stage-1	Stage-1 & 2	Stage-1 & 2	Stage-1 & 2
DERA Coordination	X	X	O	O
Internal Price	Wholesale price	Pricing function	Wholesale price	Pricing function

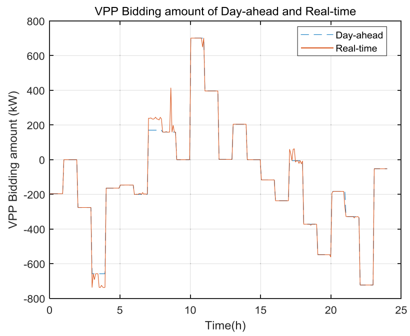

FIGURE 5. Case 1: VPP operation result in DAM/RTM.

who fail to comply with the DAM schedule in real time will have less profits or more costs.

In both of Case 3-1 and Case 3-2, the proposed method is applied so that the DERA adjusts the internal bid quantity in the DAM considering the errors between the DAM and the RTM. The DERA adjusts its internal bid quantity through iterations. The only difference is that the price applied to the DERA is the wholesale price in Case 3-1 and the price by the pricing function in Case 3-2. The effectiveness of the pricing function can be confirmed through comparing Case 1 and Case 2 results. The responsiveness of the DERAs in real time can be confirmed through comparing Case 2 and Case 3-2. Here, the MG is able to adjust its own bids because only the MG is assumed to have its own ESS. In the case of the EVA and the DRA, the bid quantity cannot be adjusted as intended because they only have entrusted resources.

C. BIDDING RESULTS OF CASE 1 AND CASE 2

Fig. 5 shows the operational results of the VPP for the DAM and the RTM. The DAM results show that scheduled purchase (or charging) value in negative and sales (or discharging) value in positive are based on the price curve. That is, selling bids are applied only during higher price times, and purchasing bids are applied during lower price times. It also shows the results of responding to uncertainty for complying with the DAM schedule in a real-time environment.

In Fig. 6, forecast errors occur in the PV and the load of each participant, and the ESS repeatedly recalculate the RTM bid every 5 minute to comply with errors. Fig. 6-(c) shows that the ESS output has changed to cope with the uncertainty in the real-time environment. Accordingly, it can be seen that ESS SOC in Fig. 6-(d) is also changed from the results expected on the previous day. Fig. 7 shows the bidding results of the MG

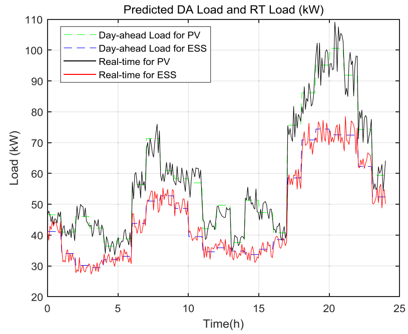

(a) Case 1: Load results of PV and ESS

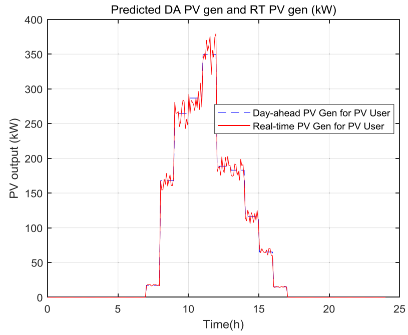

(b) Case 1: PV output results.

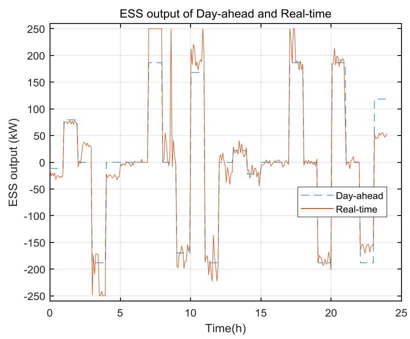

(c) Case 1: ESS output results.

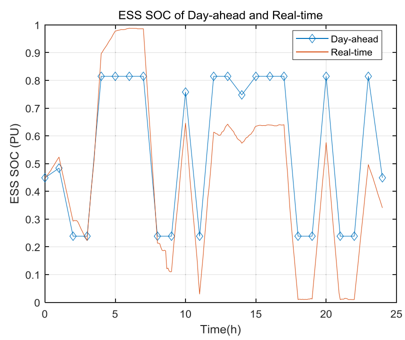

(d) Case 1: ESS SOC results.

FIGURE 6. Case 1 simulation results of ESS, PV in DAM/RTM.

in the DAM and the RTM. As mentioned earlier, because only the MG is assumed to have the ESS, the MG can comply with the DAM schedule in response to changes in the PV and load by adjusting the ESS output power, as shown in Fig. 7-(a). As a result, the ESS SOC differs from the result based on

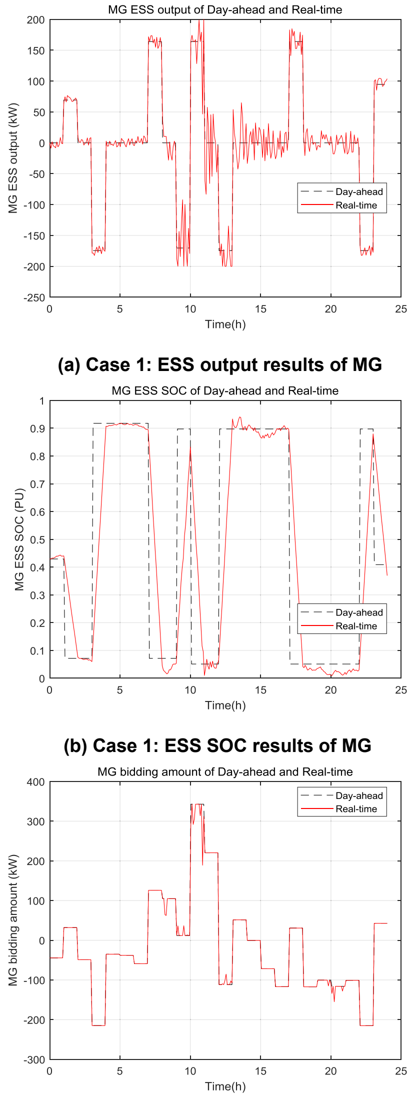

(a) Case 1: ESS output results of MG

(b) Case 1: ESS SOC results of MG

(c) Case 1: bidding results of MG

FIGURE 7. Case 1 simulation results of MG in DAM/RTM.

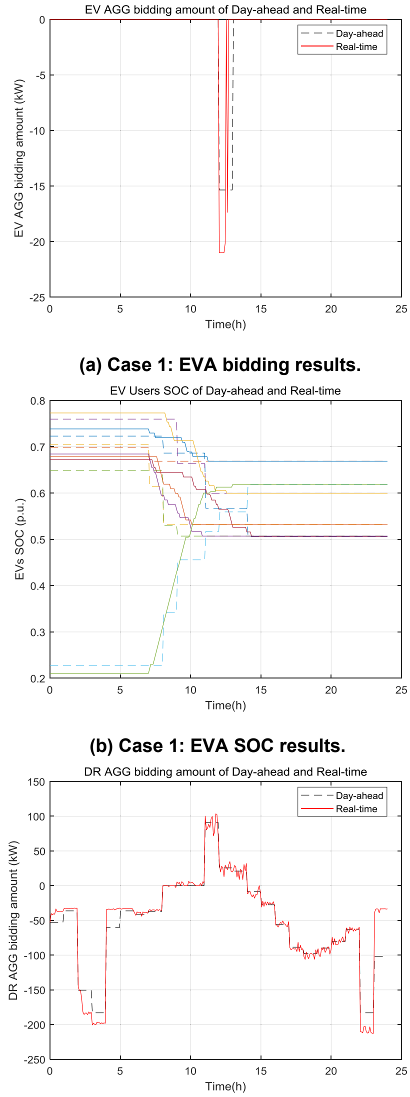

(a) Case 1: EVA bidding results.

(b) Case 1: EVA SOC results.

(c) Case 1: DRA bidding results.

FIGURE 8. Case 1 simulation results of EVA, DRA in DAM/RTM.

the day-ahead values. The MG tries to comply with the DAM schedule as much as possible, but failed to comply at some time due to lack of reserve energy to cope with uncertainty.

In the case of the EVA and DRA, the optimal results are derived according to the parameters such as entry/exit time and SOC of the EVs, the PV and the load prediction values of users participating in DR, which is changed by re-forecasting every 5 minute. Thus, Figs. 8-(a) and (b) show that the differences between the real-time output and DAM schedule are relatively large. In Fig. 8-(b), the dotted line represents the day-ahead SOC values of the EVs and the solid line represents the SOC values of the EVs in real time. In the case of the EVA, because there has been uncertainty about the entry and exit of the EVs, the RTM bidding results were changed by determining charging at a better time considering the conditions of unexpectedly early or delayed exit of some EVs. The reason why the EVA simply carried out purchase bidding is that it was a solution to satisfy the EVs' requirements without selling in consideration of the SOC conditions at the entry/exit time of the EVs.

In the case of the DRA, differences from the DAM schedule occurs because the parameters of the next day are taken into account when determining the RTM bid quantity, as well as factors due to uncertainties in the PV and the load of users participating in the DR. It seems that the result of increasing purchase bidding is slightly higher at night when the prices are relatively low. This can be seen as a result derived though the rolling horizon technique.

Although many deviations occur owing to real-time forecast errors of the PV, there are no significant fluctuations in the VPP's total bid quantity because the ESS and the MG ESS adjust their output as much as possible and suppress the fluctuations. From the ESS output and SOC result of the MG in Fig. 7, it can be seen that the SOC reached the lower limits

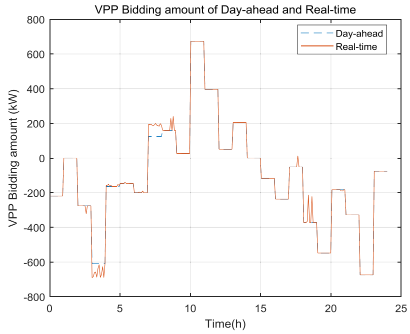

FIGURE 9. Case 3: VPP operation result in DAM/RTM.

at 11h and 20h and the ESS output could not be dispatched as intended. Accordingly at 9h-11h, 13h, and 20h-21h the MG cannot comply with the DAM schedule. That is, scheduling every 5 min. is conducted through considering all fluctuations for the next 24 hours, however, additional purchases and sales were performed because charging/discharging was not possible owing to the physical limits of the ESS.

Two conclusions can be drawn from these results. First, to manage real-time uncertainty, dispatchable resources such as ESS are required. Second, even if the dispatchable resources are equipped, when the schedule is configured to maximize the profits or minimize the costs of the DAM without considering the real-time uncertainty, the real-time uncertainty cannot be properly managed. Therefore, each participant needs to configure a bidding schedule to manage real-time uncertainty when determining the internal DAM bidding.

In Case 2, no differences with Case 1 in the internal bid are made except the costs and profits of each participant calculated by the VPP operator. On the other hand, in Case 3-1 and Case 3-2, the adjustments in the internal DAM bid of the MG is identified when the coordination is applied according to the proposed strategy. No differences between Case 3-1 and Case 3-2 are made except the costs and profits as well. Comparisons between all cases are presented in Section IV-E.

D. BIDDING RESULT OF CASE 3-1 AND CASE 3-2

Case 3-1 and Case 3-2 shows the results of the operation of the MG with adjusting the range of its internal bid through an iterative process.

Comparing Fig. 5 in Case 1 to Fig. 9, the VPP's DAM bid has decreased because the MG has repeatedly adjusted the internal bid to manage real-time fluctuation. Table 4 representing the difference of average bid quantity in kWh between the day-ahead schedule result and the real-time result also shows that the MG responded to uncertainty better than Case 1. The smaller this value, the better the day-ahead schedule is fulfilled.

As to the EVA, the differences is same as Case 1 since there was no change in the bid quantity. In the result of the DRA, the difference of average bid quantity has decreased as the VPP's capability to manage real-time uncertainty increased due to the MG's bid quantity adjustments. In Fig. 10, the VPP's capability of managing fluctuation is improved through real-time charging/discharging of the ESS controlled by the VPP, and also as the MG responds to real-time fluctuation.

TABLE 4. Difference of average bid quantity between day-ahead and real-time results.

Unit : kWh

Entity / Case	VPP	MG	EVA	DRA
Case 1	16.18	8.79	3.48	9.41
Case 3-1	15.73	3.13	3.48	8.23

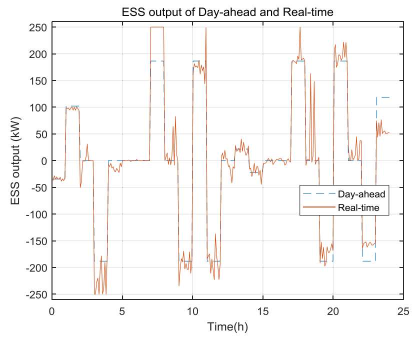

(a) Case 3: ESS output results.

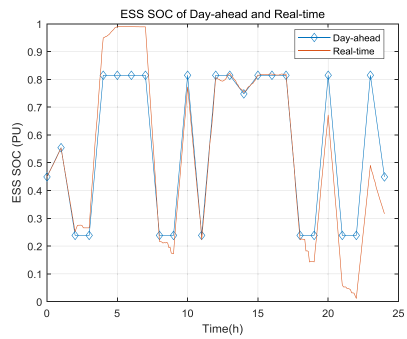

(b) Case 3: ESS SOC results.

FIGURE 10. Case 3: Simulation Results of ESS in DAM/RTM.

Fig. 11 shows the MG operation results where the adjustment is applied and the DAM bid quantity is finally converged. Because the MG ESS has reserve energy to sufficiently respond to real-time fluctuation, time duration exceeding the SOC limit is reduced. As a result of satisfying most of the DAM schedule, the MG will be paid based on the wholesale market price, thereby obtaining the maximum profits.

Fig. 12 and Fig. 13 show the SOC upper/lower limits and differences of errors between the DAM schedule and the real-time response of the MG ESS through the iterative process respectively. When the error between the DAM schedule and the real-time response occurs, the MG receives feedback from the VPP and adjusts the upper and lower limits of its own ESS according to the proposed strategy. At the beginning of the iteration, the DAM bid is calculated without considering real-time fluctuation. Thus, errors occur due to the failure of complying with real-time fluctuation. Through the iteration processes, real-time responsiveness are guaranteed owing to

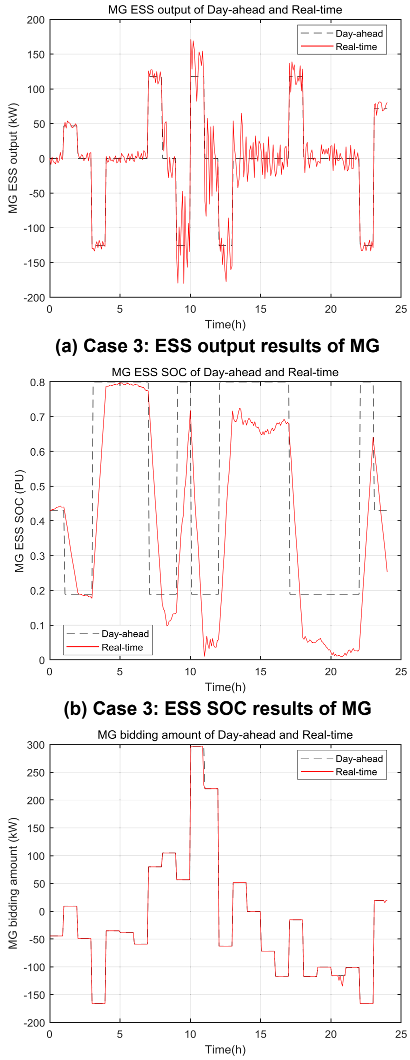

FIGURE 11. Case 3: MG operation results in DAM/RTM.

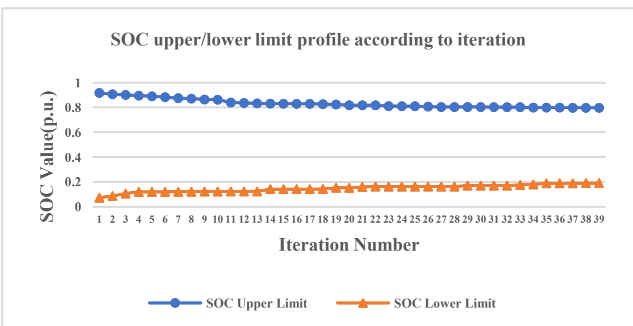

FIGURE 12. MG ESS SOC upper/lower limit adjustment result.

additional energy reserves, and the errors gradually disappear. Because not all participants can fully respond to fluctuation, it is inappropriate to set the size of the error as a criterion for stopping iteration. Instead, a difference of errors is used. If the difference remains at a certain level, additional reserves are no longer required. Here, the reference value for stopping iteration is set to 0.001.

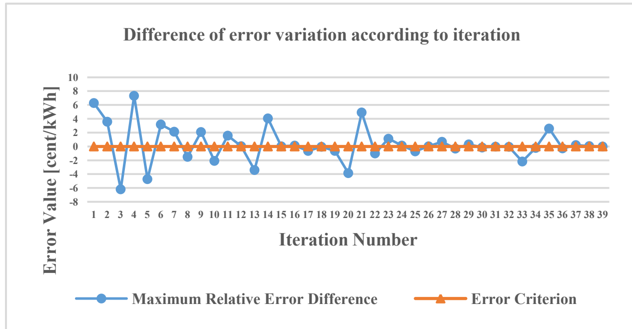

FIGURE 13. Differences in errors between the DAM bidding and RTM response according to the iteration.

It can be explained in two ways that there is no variation in the difference of errors. First, even if the bid quantity is adjusted further, there may be a certain level of error due to physical limitations. Second, the lower bidding range further causes reduced errors, but the DAM bid quantity will be reduced according to that action, and thus the cost or profit for bidding quantity will be adjusted. In other words, the former is physically impossible to coordinate, and the latter focuses on the DAM profit. As a result, because the adjustment of the bid quantity through the iteration process is determined by the step size (ε), the adjusted bid affects the optimal point when the adjustment by the VPP's feedback is repeated once. Because the adjustment process can be achieved through receiving actual operational data, it can be gradually corrected by interactions with participants as time passes, even if a somewhat insufficient result is initially produced.

E. COST AND PROFIT COMPARISON

In this section, the cost comparison of each participant and the profit comparison of the VPP between Case 1 and Case 2 is presented. The cost and profit comparison between Case 3-1 and Case 3-2 is presented in the same way. This paper assume that the all of the VPP's profits through transaction with the energy market are basically allocated to each participants while the VPP tries to obtain maximum profits. That is, the VPP's own profits are supposed to be zero. Instead, the VPP can earn a kind of transaction fee according to specific contracts with each participants.

When applying the proposed methodology, however, the participants may get a penalty based on responsiveness to the real-time dispatch signal by the VPP. The VPP operator may earn the profits as much as the penalty.

Table 5 shows the cost of each participant and the profit of the VPP operator for each case. All participants basically have reduced costs by participating in the VPP. As mentioned above, the VPP's own profit is zero in Case 1 and Case 3-2. The sum of the costs of each participant and the cost of the VPP are not same because the results also included one PV and one energy storage system for which the VPP has operation authority. In real time, additional purchasing and selling bids are processed to buy at a higher price and sell at a lower price by the weight factor. For example, if the weight

TABLE 5. Total cost/profit result of participants/VPP in case study.

Unit : USD

Items / Case	Day-ahead cost				Real-time cost				VPP's own profit
	MG	EVA	DRA	VPP	MG	EVA	DRA	VPP	
Without VPP	290.07	4.37	468.97	0	298.49	3.38	455.45	0	0
With VPP (Case 1)	140.88	3.87	360.33	741.26	150.75	3.00	350.92	727.86	0
With VPP (Case 2)	143.76	3.99	373.91	724.68	153.54	3.08	360.45	715.46	12.399
With VPP (Case 3-1)	150.68	3.87	360.33	759.67	153.32	3.00	361.58	750.35	0
With VPP (Case 3-2)	151.22	3.99	372.53	746.81	153.86	3.08	372.91	738.40	11.954

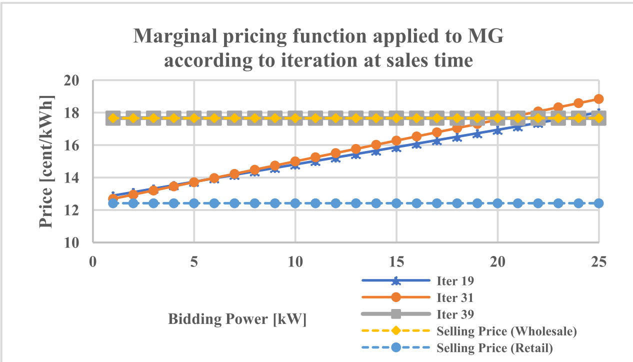

FIGURE 14. Marginal pricing function at sales time for MG according to iteration.

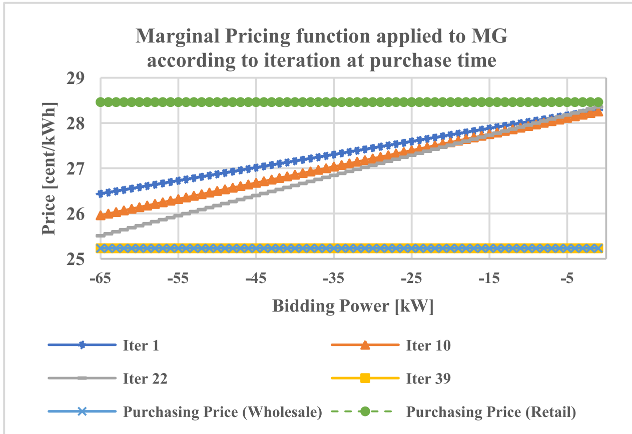

FIGURE 15. Marginal pricing function at purchase time for MG according to iteration.

factor is 0.2, energy must be purchased at a price 20% higher than the DAM price in RTM, and must be sold at a 20% lower price. In case of the MG, the cost in real time is higher than that of day-ahead. For the EVA and the DRA, the cost results in real time are lower, as the bid quantity has been decreased due to real-time fluctuation of uncertainty resources. It means that the cost has been decreased by reducing the purchased bid quantity during the purchasing bid time period.

In Case 2, each participant's cost increased compared to Case 1 because internal price was applied. That is, they buy at a price higher than the wholesale market price for a purchase bid and sell at a price lower than the wholesale market price for a sales bid. As a result, the VPP could earn the same profits as much as the increased costs of each participants, resulting in a profit of about $12.40.

Fig. 14 and Fig. 15 show the first derivative of the pricing function for the MG's purchasing bid time and selling bid time according to iteration.

In the case of the purchase bidding time, since a negative sign is applied to the bid quantity, the x-axis is designated as a negative number. As the iteration progresses, the MG's bid quantity is adjusted and the pricing function is adjusted accordingly. Therefore, the pricing function is not derived as a quadratic equation at every time and every iteration. The results of the iteration number derived from the quadratic equation of the pricing function are summarized in the graph below. As mentioned earlier, the graphs below show the first derivative of the pricing function. In the graph of the sales time period, it can be seen that the selling price increases for the same quantity of bid as the iteration passes. On the other hand, in the graph of the purchasing time period, it can be seen that the purchase price decreases for the same quantity of bidding as the iteration passes. In other words, the MG's bid quantity adjustment improves the responsiveness to uncertainty, which means that the MG is able to get the profit at a higher price or purchase cost at a lower price. Finally, if the real-time operation result conforms to the day-ahead schedule, the error disappears and the price made by the pricing function becomes the wholesale market price.

In Case 3-1 and Case 3-2, the DRA's bidding results changed according to the bid quantity of the MG for the DAM. In the case of the EVA, the bidding result did not change because the SOC of available EVs and the SOC of entry and exit of the EVs did not change. In the adjusted results, the DRA has higher costs in real time because they made additional purchases of sales. The MG's responsiveness to the real-time uncertainty was high by adjusting the bid quantity. Therefore, no significant changes are seen when comparing the MG's real-time cost. The VPP's profits are also reduced. Consequently, if all of the participants can comply with their day-ahead schedule in real-time environment, the proposed methodology can have an advantage of managing most of the real-time uncertainties properly although the VPP's profits may be decreased.

Fig. 16 shows total cost of the VPP. As mentioned earlier, all these costs are borne by the participants. The lower cost in the RTM compared to the DAM means that the RTM bid quantity of the VPP is reduced compared to that of the

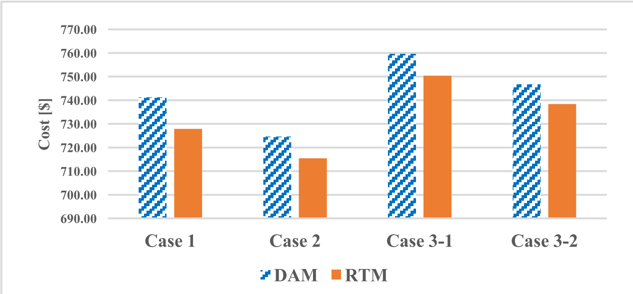

FIGURE 16. Total cost result of VPP in DAM/RTM.

TABLE 6. Increased cost of participants and decreased profit of VPP according to weight factor.

Entity \ Weight		0.2	0.5	0.9
MG Cost	Case 1 & Case 2	2.7855	2.7688	2.7467
	Case 3-1 & Case 3-2	0.5370	0.5386	0.5406
EVA Cost	Case 1 & Case 2	0.0869	0.0869	0.0869
	Case 3-1 & Case 3-2	0.0869	0.0869	0.0869
DRA Cost	Case 1 & Case 2	9.5267	7.9762	8.1263
	Case 3-1 & Case 3-2	11.3301	10.0749	10.2730
VPP Profit	Case 1 & Case 2	12.3991	10.8319	10.9599
	Case 3-1 & Case 3-2	11.9540	10.7004	10.9006

DAM. The actual profits of the VPP operator by the pricing function is as much as the difference between the RTM costs in Case 1 and Case 2, or as much as the difference between the RTM costs in Case 3-1 and Case 3-2. These benefits are derived from the cost of penalty imposed on the participants.

Table 6 shows the cost difference between Case 1 and Case 2, and between Case 3-1 and Case 3-2 for each participant. It shows the cost trend by the proposed pricing function according to the price weight factor in the RTM. Positive numbers mean an increase in cost/profit. First, in the case of the MG and the EVA, no change in the bid quantity was shown regardless of the change in weight factor. This means that there were no resources to have capability to change the bid even if the price was increased by the weight factor. In the case of the MG, because the price is set to the same rate for each time period, the MG has no incentive to adjust its ESS schedule even though the bid quantity must be adjusted using its ESS resource. The EVA did not adjust its schedule because it did not have authority to adjust EVs schedule, resulting in no change according to the weighted price. And also the EVA did not have cost difference because no additional purchases or sales were performed in the RTM. However, in the case of the MG, the cost difference tended to decrease even though there were no change in the real-time bid quantity. This is due to the internal price by the VPP's pricing function calculated by time. Because the internal price was calculated according to the fluctuation that occurred over time, the difference from the wholesale market price was not constant by time. For example, on the other hand, if a penalty of 2 cent is applied to the wholesale market price in all purchase and sales time periods by the pricing function,

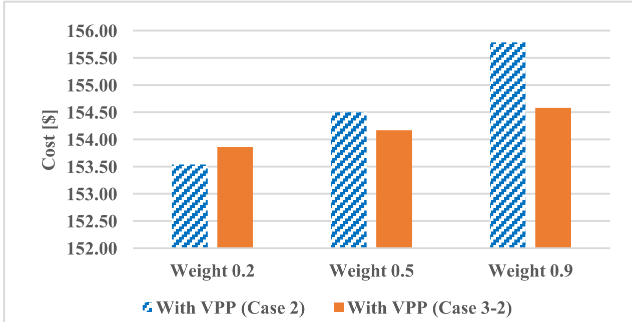

FIGURE 17. Example of degree of increasing cost according to weight factor.

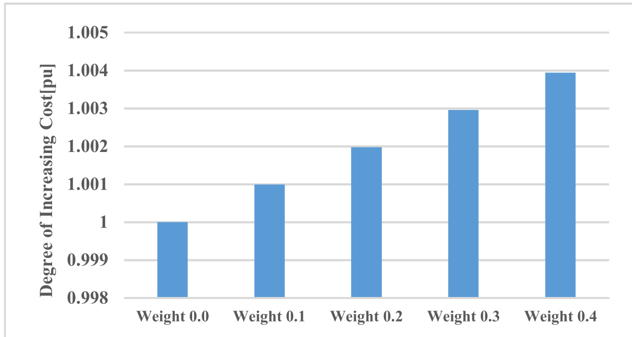

FIGURE 18. Total cost of MG between case 2 and 3-2 according to weight factor.

the cost reduction increases as the weight factor increased. Fig. 17 shows the example case.

Since applied penalties for each time period are different, the cost increase or decrease depend on the weight factor event if the quantity does not change. This can be seen by looking at the results of the first and second rows of Table 6. In Case 1 and Case 2 of the MG, the cost difference has a decreasing trend. In Case 3-1 and Case 3-2 of the MG, the cost difference has an increasing trend. Though these are not a big differences, it means that the weight factors do not dominantly affect the cost increase. The internal price change due to the fluctuation derived over time has some influences.

In the case of the DRA, the cost difference decreased as the weight factor increased. It means that the DRA's real-time operation was adjusted according to the weight factor and thus the DRA adhered its day-ahead schedule more. In other words, it means that the penalty impact has been reduced. However, at the weight of 0.9, it can be seen that the cost difference slightly increased, which means that the effect of the weight increase slightly. In addition, because the internal price calculation is not linear, the cost difference trend according to the weight increase appears differently. However, if the cost calculated by the proposed pricing function is increased compared to the original case, and the responsiveness of coping with real-time fluctuation is high, the cost difference is small. It means that the proposed pricing function is applied as intended.

Fig. 18 shows the cost between Case 2 and Case 3-2 of the MG according to the real-time price weight factors. It can be seen that the larger the weight factors, the smaller the cost of

Case 3-2 is than that of Case 2. This implicates that the MG's option to prepare reserve energy for real-time uncertainty by adjusting the day-ahead bid quantity can reduce the cost due to less penalty.

Through the above results the VPP can establish an optimal DAM bidding strategy to have more responsiveness to fluctuation in a real-time, and the participants in the VPP can manage real-time uncertainty by themselves so that the VPP can faithfully achieve its own purpose. If all participants of the VPP can cope with uncertainties in real time, a more efficient distribution network operation can also be possible.

V. CONCLUSION AND FUTURE STUDIES

VPP technologies continue to develop as a way to cope with uncertainty caused by the increasing deployment of various DERs in an electric power system. If the uncertainty inherent in VPP participants, that is, DERs, is not well managed, side effects such as an unbalanced supply and demand of the power grid and deterioration in the power quality may occur, and the feasibility of the VPP may also deteriorate. In this paper, the optimal operation strategy of the VPP is proposed considering the real-time dispatch uncertainty of the DERA. The DERA's responsiveness to real-time uncertainty is evaluated continuously by the VPP on a daily basis. Based on the DERA's real-time responsiveness evaluation results, the VPP transmits the day's error result to the DERA and determines the internal price of the DERA by the proposed pricing function. According to the error result, the DERA adjust its energy reserve for the next DAM internal bid. They repeat the process again for the next day. Using this iteration process, an operation strategy that manages real-time uncertainty in the DERA while satisfying their maximum profit can be established. In other words, defining the DERA pricing function as the cost that the VPP pays to the DERA and updating the parameters of the pricing function continuously according to the real-time responsiveness of the DERA to the DAM schedule can establish a coordination process between the VPP and DERA, and thus the real-time responsiveness of the DERA can be increased. The effectiveness of the proposed strategy is verified by identifying a capability of the DERA to cope with real-time fluctuation through scenario-based simulations. The result shows that the VPP can reduce 1.6% of cost while the internal price applied to the DERA is close to the maximum. To increase the effectiveness of this strategy, it is necessary to strengthen the incentives obtained when the real-time response complies with the DAM schedule or the penalties imposed when the DAM schedule is not complied with.

In this study, DERAs including MG, EVA, and DRA were considered. Among them, only the MG was assumed to have capability to adjust its energy reserve. In the future, additional research is needed to develop further models for other types of the DERAs. In addition, when updating the parameters of the pricing function, using artificial intelligence techniques such as reinforcement learning is required to achieve more effective results.

REFERENCES

[1] *REN21, Renewables 2020 Global Status Report*, REN21 Secretariat, Paris, France, 2020.

[2] H. T. Kim and S. S. Jhang, "Key technologies for stabilization of power system for successful achievement of 3020 renewable energy policy," *Trans. Korean Inst. Elect. Eng.*, vol. 67, no. 2, pp. 149–157, 2018.

[3] L. Yavuz, A. Önen, S. M. Muyeen, and I. Kamwa, "Transformation of microgrid to virtual power plant—A comprehensive review," *IET Gener., Transmiss. Distrib.*, vol. 13, no. 11, pp. 1994–2005, Jun. 2019.

[4] S. M. Nosratabadi, R.-A. Hooshmand, and E. Gholipour, "A comprehensive review on microgrid and virtual power plant concepts employed for distributed energy resources scheduling in power systems," *Renew. Sustain. Energy Rev.*, vol. 67, pp. 341–363, Jan. 2017.

[5] D. Pudjianto, C. Ramsay, and G. Strbac, "Virtual power plant and system integration of distributed energy resources," *IET Renew. Power Gener.*, vol. 1, no. 1, p. 10, 2007.

[6] *Virtual Power Plants—Part 1: Architecture and Functional Requirements*, document IEC 63189-1 ED1, Geneva, Switzerland, 2020.

[7] *Participation of Distributed Energy Resource Aggregations in Markets Operated by Regional Transmission Organizations and Independent System Operators*, document FERC 2222, FERC, Washington, DC, USA, 2020.

[8] S. Yu, F. Fang, Y. Liu, and J. Liu, "Uncertainties of virtual power plant: Problems and countermeasures," *Appl. Energy*, vol. 239, pp. 454–470, Apr. 2019.

[9] S. Rahmani-Dabbagh and M. K. Sheikh-El-Eslami, "A profit sharing scheme for distributed energy resources integrated into a virtual power plant," *Appl. Energy*, vol. 184, pp. 313–328, Dec. 2016.

[10] M. A. Hannan, M. G. M. Abdolrasol, M. Faisal, P. J. Ker, R. A. Begum, and A. Hussain, "Binary particle swarm optimization for scheduling MG integrated virtual power plant toward energy saving," *IEEE Access*, vol. 7, pp. 107937–107951, 2019.

[11] W. Tang and H.-T. Yang, "Optimal operation and bidding strategy of a virtual power plant integrated with energy storage systems and elasticity demand response," *IEEE Access*, vol. 7, pp. 79798–79809, 2019.

[12] S. I. Taheri, M. B. C. Salles, and E. C. M. Costa, "Optimal cost management of distributed generation units and microgrids for virtual power plant scheduling," *IEEE Access*, vol. 8, pp. 208449–208461, 2020.

[13] J. Hu, C. Jiang, and Y. Liu, "Short-term bidding strategy for a price-maker virtual power plant based on interval optimization," *Energies*, vol. 12, no. 19, p. 3662, Sep. 2019.

[14] H. T. Nguyen, L. B. Le, and Z. Wang, "A bidding strategy for virtual power plants with the intraday demand response exchange market using the stochastic programming," *IEEE Trans. Ind. Appl.*, vol. 54, no. 4, pp. 3044–3055, Jul. 2018.

[15] A. T. Al-Awami, N. A. Amleh, and A. M. Muqbel, "Optimal demand response bidding and pricing mechanism with fuzzy optimization: Application for a virtual power plant," *IEEE Trans. Ind. Appl.*, vol. 53, no. 5, pp. 5051–5061, Sep. 2017.

[16] M. Yazdaninejad, N. Amjady, and S. Dehghan, "VPP self-scheduling strategy using multi-horizon IGDT, enhanced normalized normal constraint, and bi-directional decision-making approach," *IEEE Trans. Smart Grid*, vol. 11, no. 4, pp. 3632–3645, Jul. 2020.

[17] E. Mashhour and S. M. Moghaddas-Tafreshi, "Bidding strategy of virtual power plant for participating in energy and spinning reserve markets—Part I: Problem formulation," *IEEE Trans. Power Syst.*, vol. 26, no. 2, pp. 949–956, May 2011.

[18] N. Naval, R. Sánchez, and J. M. Yusta, "A virtual power plant optimal dispatch model with large and small-scale distributed renewable generation," *Renew. Energy*, vol. 151, pp. 57–69, May 2020.

[19] H. Bai, S. Miao, X. Ran, and C. Ye, "Optimal dispatch strategy of a virtual power plant containing battery switch stations in a unified electricity market," *Energies*, vol. 8, no. 3, pp. 2268–2289, Mar. 2015.

[20] F. Luo, Z. Y. Dong, K. Meng, J. Qiu, J. Yang, and K. P. Wong, "Short-term operational planning framework for virtual power plants with high renewable penetrations," *IET Renew. Power Gener.*, vol. 10, no. 5, pp. 623–633, May 2016.

[21] H. Pandžic, J. M. Morales, A. J. Conejo, and I. Kuzle, "Offering model for a virtual power plant based on stochastic programming," *Appl. Energy*, vol. 105, pp. 282–292, May 2013.

[22] S. R. Dabbagh and M. K. Sheikh-El-Eslami, "Risk-based profit allocation to DERs integrated with a virtual power plant using cooperative game theory," *Electr. Power Syst. Res.*, vol. 121, pp. 368–378, Apr. 2015.

[23] Y. Wang, X. Ai, Z. Tan, L. Yan, and S. Liu, "Interactive dispatch modes and bidding strategy of multiple virtual power plants based on demand response and game theory," *IEEE Trans. Smart Grid*, vol. 7, no. 1, pp. 510–519, Jan. 2016.

[24] M. Pasetti, S. Rinaldi, and D. Manerba, "A virtual power plant architecture for the demand-side management of smart prosumers," *Appl. Sci.*, vol. 8, no. 3, p. 432, Mar. 2018.

[25] L. Lin, X. Guan, Y. Peng, N. Wang, S. Maharjan, and T. Ohtsuki, "Deep reinforcement learning for economic dispatch of virtual power plant in Internet of energy," *IEEE Internet Things J.*, vol. 7, no. 7, pp. 6288–6301, Jul. 2020.

[26] H. Khaloie, M. Mollahassani-Pour, and A. Anvari-Moghaddam, "Optimal behavior of a hybrid power producer in day-ahead and intraday markets: A bi-objective CVaR-based approach," *IEEE Trans. Sustain. Energy*, vol. 12, no. 2, pp. 931–943, Apr. 2021.

[27] M. Vahedipour-Dahraie, H. Rashidizadeh-Kermani, A. Anvari-Moghaddam, and P. Siano, "Risk-averse probabilistic framework for scheduling of virtual power plants considering demand response and uncertainties," *Int. J. Electr. Power Energy Syst.*, vol. 121, Oct. 2020, Art. no. 106126.

[28] H. Khaloie, A. Abdollahi, M. Shafie-Khah, P. Siano, S. Nojavan, A. Anvari-Moghaddam, and J. P. S. Catalão, "Co-optimized bidding strategy of an integrated wind-thermal-photovoltaic system in deregulated electricity market under uncertainties," *J. Cleaner Prod.*, vol. 242, Jan. 2020, Art. no. 118434.

[29] H. Khaloie, A. Abdollahi, M. Shafie-Khah, A. Anvari-Moghaddam, S. Nojavan, P. Siano, and J. P. S. Catalão, "Coordinated wind-thermal-energy storage offering strategy in energy and spinning reserve markets using a multi-stage model," *Appl. Energy*, vol. 259, Feb. 2020, Art. no. 114168.

[30] H. Khaloie, A. Anvari-Moghaddam, N. Hatziargyriou, and J. Contreras, "Risk-constrained self-scheduling of a hybrid power plant considering interval-based intraday demand response exchange market prices," *J. Cleaner Prod.*, vol. 282, Feb. 2021, Art. no. 125344.

[31] H. Lee, G.-S. Byeon, J.-H. Jeon, A. Hussain, H.-M. Kim, A. O. Rousis, and G. Strbac, "An energy management system with optimum reserve power procurement function for microgrid resilience improvement," *IEEE Access*, vol. 7, pp. 42577–42585, 2019.

[32] M. A. Ortega-Vazquez, F. Bouffard, and V. Silva, "Electric vehicle aggregator/system operator coordination for charging scheduling and services procurement," *IEEE Trans. Power Syst.*, vol. 28, no. 2, pp. 1806–1815, May 2013.

[33] *Settlement Intervals and Shortage Pricing in Markets Operated by Regional Transmission Organizations and Independent System Operators*, document FERC 825, FERC, Washington, DC, USA, 2016.

[34] *PJM Market Home Page*. Accessed: Dec. 12, 2019. [Online]. Available: https://www.pjm.com/

JINHO LEE received the B.S. degree in physics from Pusan National University, Busan, South Korea, in 2006, and the M.S. degree in energy studies from Ajou University, Suwon, South Korea, in 2010. He is currently pursuing the Ph.D. degree in electrical engineering with Inha University, Incheon, South Korea. Since 2010, he has been working with the Research and Development Center, Hyosung Corporation, where he is the Chief Researcher. His research interests include energy storage systems, microgrids, and virtual power plant operation.

DONGJUN WON received the B.S., M.S., and Ph.D. degrees in electrical engineering from Seoul National University, Seoul, South Korea, in 1998, 2000, and 2004, respectively. He was previously a Postdoctoral Fellow with the APT Center, University of Washington, Seattle. He is currently a Professor with the Department of Electrical Engineering, Inha University, Incheon, South Korea. His research interests include microgrids, renewable energy, electric vehicles, and energy storage systems.